

# Mitofusin 2 is necessary for striatal axonal projections of midbrain dopamine neurons

Seungmin Lee<sup>1</sup>, Fredrik H. Sterky<sup>1</sup>, Arnaud Mourier<sup>3</sup>, Mügen Terzioglu<sup>3</sup>, Staffan Cullheim<sup>2</sup>, Lars Olson<sup>2</sup> and Nils-Göran Larsson<sup>1,3,\*</sup>

<sup>1</sup>Department of Laboratory Medicine, and <sup>2</sup>Department of Neuroscience, Karolinska Institutet, Retzius väg 8, SE-171 77 Stockholm, Sweden, <sup>3</sup>Max Planck Institute for Biology of Ageing, Gleueler Str. 50a, 50931 Cologne, Germany

Received July 21, 2012; Revised and Accepted August 16, 2012

Mitochondrial dysfunction is implicated in aging and degenerative disorders such as Parkinson's disease (PD). Continuous fission and fusion of mitochondria shapes their morphology and is essential to maintain oxidative phosphorylation. Loss-of-function mutations in *PTEN-induced kinase1* (*PINK1*) or *Parkin* cause a recessive form of PD and have been linked to altered regulation of mitochondrial dynamics. More specifically, the E3 ubiquitin ligase Parkin has been shown to directly regulate the levels of mitofusin 1 (*Mfn1*) and *Mfn2*, two homologous outer membrane large GTPases that govern mitochondrial fusion, but it is not known whether this is of relevance for disease pathophysiology. Here, we address the importance of *Mfn1* and *Mfn2* in midbrain dopamine (DA) neurons *in vivo* by characterizing mice with DA neuron-specific knockout of *Mfn1* or *Mfn2*. We find that *Mfn1* is dispensable for DA neuron survival and motor function. In contrast, *Mfn2* DA neuron-specific knockouts develop a fatal phenotype with reduced weight, locomotor disturbances and death by 7 weeks of age. *Mfn2* knockout DA neurons have spherical and enlarged mitochondria with abnormal cristae and impaired respiratory chain function. Parkin does not translocate to these defective mitochondria. Surprisingly, *Mfn2* DA neuron-specific knockout mice have normal numbers of midbrain DA neurons, whereas there is a severe loss of DA nerve terminals in the striatum, accompanied by depletion of striatal DA levels. These results show that *Mfn2*, but not *Mfn1*, is required for axonal projections of DA neurons *in vivo*.

## INTRODUCTION

Parkinson's disease (PD) is a common neurodegenerative condition characterized by loss of dopamine (DA)-producing neurons in the substantia nigra pars compacta (SNc). Although other populations of neurons are also affected, the hallmark motor symptoms of PD are caused by the resulting DA deficiency in the striatum, the area to which these DA neurons project. The pathophysiological events that lead to the degeneration of DA neurons are unclear, but may involve mitochondrial dysfunction (1). A distinct form of PD, autosomal recessive juvenile parkinsonism (AR-JP), is caused by mutations in the genes *PTEN-induced kinase 1* (*PINK1*), *Parkin* and *DJ-1*. Several genes mutated in AR-JP have been linked to the regulation of mitochondrial function. The E3 ubiquitin ligase Parkin

and the mitochondrial kinase *PINK1* act in a common pathway suggested to be involved in mitochondrial quality control. In cell lines, depolarization of the membrane potential across the inner mitochondrial membrane induces a *PINK1*-dependent recruitment of cytosolic Parkin to the mitochondrial outer membrane (2). The precise role of Parkin on the outer mitochondrial surface remains to be established and the link to the degeneration of DA neurons is not well understood (3).

We have previously addressed the consequences of mitochondrial dysfunction in DA neurons by creating MitoPark mice that have DA-specific disruption of mitochondrial transcription factor A (4), a dual function protein required for mitochondrial transcription initiation and for packaging of mtDNA into nucleoids (5,6). These mice develop severe motor symptoms due to progressive loss of DA neurons in

\*To whom correspondence should be addressed at: Max Planck Institute for Biology of Ageing, Robert-Koch-Str. 21, 50931 Cologne, Germany. Tel: +49 22147889771; Fax: +49 22147897409; Email: larsson@age.mpg.de

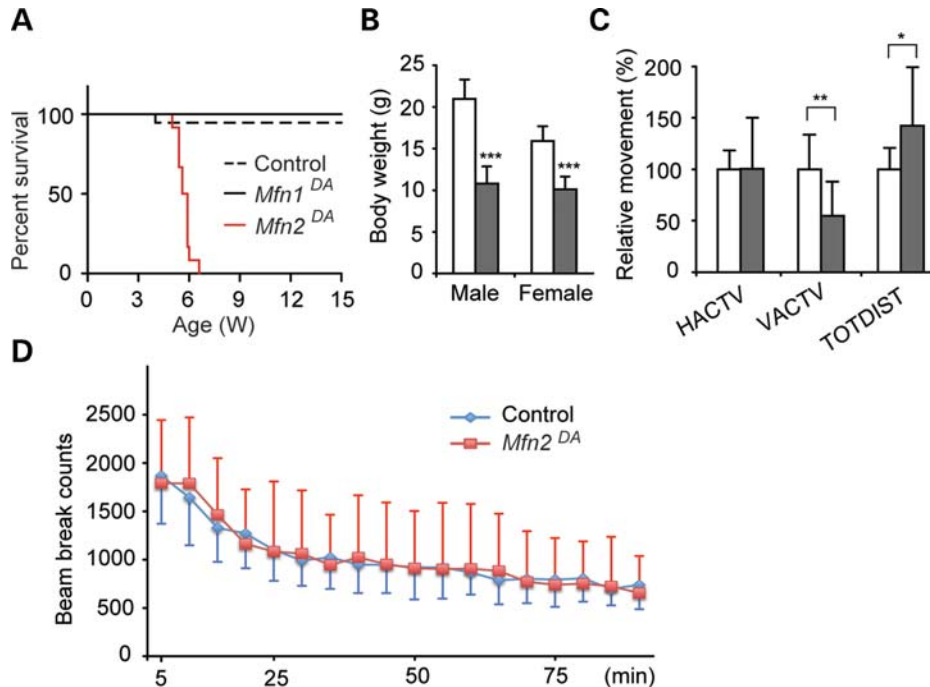


**Figure 1.** Loss of *Mfn2* but not *Mfn1* in DA neurons results in a lethal phenotype. (A) Kaplan–Meier survival curves of *Mfn1*<sup>DA</sup> and *Mfn2*<sup>DA</sup> mice. *Mfn2*<sup>DA</sup> mice ( $n = 17$ ) had a median survival age of 5.8 weeks ( $P < 0.0001$ ). (B) Body weight of control and *Mfn2*<sup>DA</sup> ( $n = 17$  for each genotype) male and female mice at 5 weeks of age. (C) Spontaneous motor function in 5-week-old control and *Mfn2*<sup>DA</sup> mice ( $n = 17$  for each genotype). Horizontal activity (locomotion, HACTV), vertical activity (rearing, VACTV) and total distance of horizontal movements (TOTDIST) were measured for 1.5 h in open-field activity cages. Open bars, control; filled bars, *Mfn2*<sup>DA</sup> mice. Error bars represent  $\pm$  SD. \* $P < 0.05$ , \*\* $P < 0.01$  and \*\*\* $P < 0.001$  by Student's two-tailed  $t$ -test. (D) Locomotion measured for 1.5 h in control (blue line) and *Mfn2*<sup>DA</sup> (red line) mice at 5 weeks of age. Data were collected every 5 min. Error bars represent  $\pm$  SD.

SNC. The degenerating DA neurons in MitoPark mice have abnormal mitochondrial ultrastructure and a fragmented mitochondrial network. Furthermore, the DA neurons in MitoPark mice develop large, dense and membranous intracellular bodies derived from abnormal mitochondria, and the supply of mitochondria to their distal axons is impaired (4,7).

Mitochondria form a functionally interconnected network in the cell by continuous fission and fusion (8,9). Mitochondrial dynamics is essential for embryonic development and studies in differentiated tissues have shown that continuous fission and fusion of mitochondria is necessary for maintaining mtDNA and oxidative phosphorylation capacity (10–12). Mutations in genes regulating mitochondrial fusion and fission cause human neurodegenerative diseases. For instance, mutations in *OPA1* cause atrophy of the optic nerve (13) and mutations in *MFN2* cause a form of hereditary motor and sensory neuropathy (14). It is believed that mitochondrial fusion contributes to maintaining function by allowing an exchange of mtDNA and other matrix components (8). Fission events fragment the mitochondrial network into smaller units to allow mitochondrial transport to different subcellular localizations, such as nerve terminals. Fission has also been reported to have a role in mitochondrial quality control as dysfunctional mitochondria are less prone to fuse with the main mitochondrial network (15) and instead may be degraded by autophagocytosis (16,17).

Two homologous large GTPases, mitofusin 1 (*Mfn1*) and *Mfn2*, govern fusion of the mitochondrial outer membrane in mammals (9,18). Studies have identified Parkin as a possible

regulator of mitofusin levels by direct ubiquitination to facilitate subsequent proteasome-mediated degradation (19,20). Consistent with this idea, the *Drosophila Mfn* homolog Marf accumulates in *Drosophila* PINK1 and Parkin mutants (21), and genetic manipulations that promote fission or decrease fusion can partially suppress *Drosophila* mutant phenotypes (22,23).

We have addressed the roles of *Mfn1* and *Mfn2* *in vivo* and report here that loss of *Mfn1* in DA neurons has no apparent effect. In contrast, loss of *Mfn2* in DA neurons causes severe mitochondrial fragmentation and enlargement accompanied by respiratory chain deficiency. Interestingly, *Mfn2* is critical for DA innervation of the striatum, as young adult knockout mice have normal numbers of DA neurons in SNC, whereas the DA nerve terminals in the striatum are almost completely absent. *Mfn2* is thus essential for DA neuron function and critical for axonal arborization.

## RESULTS

### Generation of conditional knockout mice with disruption of *Mfn1* or *Mfn2* in DA neurons

We assessed the expression of *Mfn1* and *Mfn2* mRNA in the mouse brain by *in situ* hybridization and found that transcripts of both genes were ubiquitously expressed in the mouse brain, including in midbrain DA neurons (Supplementary Material, Fig. S1, outlined regions). Next, we obtained conditional knockout alleles for *Mfn1* and *Mfn2* by gene targeting in the mouse (Supplementary Material, Fig. S2A–D). We tested

these knockout alleles by disrupting both genes in the heart by crossing *Mfn1<sup>loxP</sup>* and *Mfn2<sup>loxP</sup>* mice with *Ckmm-cre* mice (24). Disruption of *Mfn1* (genotype *Mfn1<sup>loxP</sup>/Mfn1<sup>loxP</sup>; +/Ckmm-cre*) or *Mfn2* (genotype *Mfn2<sup>loxP</sup>/Mfn2<sup>loxP</sup>; +/Ckmm-cre*) in the heart resulted in a very profound decrease in *Mfn1* and *Mfn2* mRNA (Supplementary Material, Fig. S2E and F) and protein, respectively (Supplementary Material, Fig. S2G). These results demonstrate that breeding of *Mfn1<sup>loxP</sup>* and *Mfn2<sup>loxP</sup>* mice to *cre*-expressing transgenic mice can efficiently abolish the expression of *Mfn1* and *Mfn2* in a selected tissue. With this information at hand, we proceeded to study the role of *Mfn1* and *Mfn2* in DA neurons by breeding *Mfn1<sup>loxP</sup>* and *Mfn2<sup>loxP</sup>* mice to *DAT-cre* mice. The mice with disruption of *Mfn1* in DA neurons (genotype *Mfn1<sup>loxP</sup>/Mfn1<sup>loxP</sup>; +/DAT-cre*, hereafter denoted *Mfn1<sup>DA</sup>* mice) were clinically unaffected, when followed until 1 year of age. In contrast, mice with disruption of *Mfn2* in DA neurons (genotype *Mfn2<sup>loxP</sup>/Mfn2<sup>loxP</sup>; +/DAT-cre*, hereafter denoted *Mfn2<sup>DA</sup>* mice) had a drastically shortened life span and died before the age of 7 weeks (median survival, 5.8 weeks; Fig. 1A). The *Mfn1<sup>DA</sup>* mice had normal body weight (Supplementary Material, Fig. S3A), whereas the *Mfn2<sup>DA</sup>* mice had reduced body weight at the age of 5 weeks (Fig. 1B). We found no differences in spontaneous locomotion or rearing in *Mfn1<sup>DA</sup>* mice in comparison with controls (Supplementary Material, Fig. S3B and C). In contrast, the *Mfn2<sup>DA</sup>* mice had significantly decreased rearing activity (Fig. 1C), whereas locomotion, assessed as horizontal beam breaks, was unchanged (Fig. 1C and D). The total distance traveled was significantly increased in *Mfn2<sup>DA</sup>* mice (Fig. 1C). Increased total distance with similar amounts of horizontal beam breaks can result from increased diagonal locomotion across the cage floor, possibly reflecting increased stress. As the decreased rearing activity of *Mfn2<sup>DA</sup>* mice may prevent them from reaching food on the cage top, a cohort of mice were provided moist food on the cage floor. Despite this, *Mfn2<sup>DA</sup>* mice continued to lose weight, became severely hypokinetic and had to be sacrificed at 11–12 weeks of age due to poor general condition (data not shown).

### Loss of *Mfn2* in DA neurons causes severe respiratory chain deficiency without recruitment of Parkin to the defective mitochondria

Next, we investigated the number of midbrain DA neurons by immunolabeling to detect tyrosine hydroxylase (TH) expression (Fig. 2A). We quantified SNc DA neurons by stereology and found normal numbers of neurons in both *Mfn1<sup>DA</sup>* (Fig. 2B) and *Mfn2<sup>DA</sup>* mice (Fig. 2C) at 5 weeks of age.

To assess mitochondrial morphology in DA neurons, we used the *lox-Stop-lox-mito-YFP* reporter mice in conjunction with the *DAT-cre* allele, as described previously (7). The mitochondrial morphology was normal in *Mfn1<sup>DA</sup>* mice at the age of 6 and 18 weeks (Fig. 3A). In contrast, the mitochondria in *Mfn2<sup>DA</sup>* mice were spherical and enlarged (Fig. 3B). These abnormal mitochondria were immunoreactive with antibodies against the mitochondrial matrix protein superoxide dismutase 2 (SOD2) and the outer mitochondrial membrane protein TOM20 (Fig. 3C), demonstrating at least some preservation of function. We also performed electron microscopy of DA neurons in *Mfn2<sup>DA</sup>* mice and found abnormal, rounded mitochondria with disorganized cristae (Fig. 3D), having a size

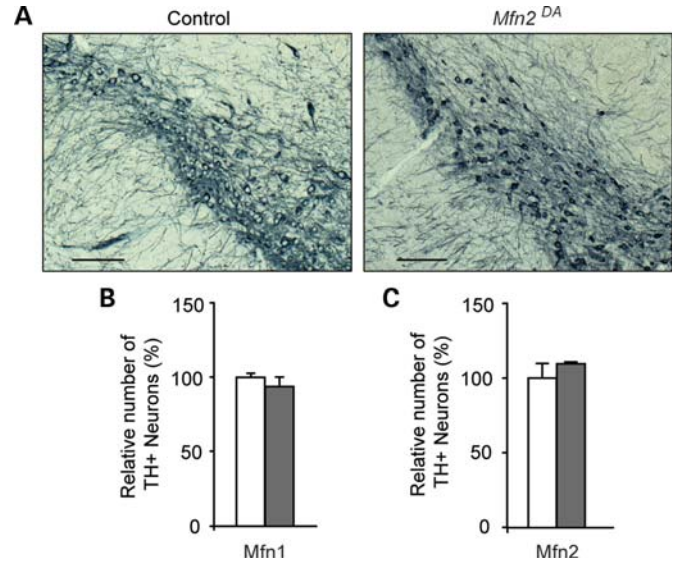


**Figure 2.** No loss of DA neurons in *Mfn1<sup>DA</sup>* or *Mfn2<sup>DA</sup>* mice. (A) TH immunoreactive DA neurons in SNc of control and *Mfn2<sup>DA</sup>* mice (scale bar: 200  $\mu$ m). (B) Relative number of TH-positive neurons in the midbrain of *Mfn1<sup>DA</sup>* mice at 5 weeks of age. Open bars, control ( $n = 3$ ); filled bars, knockout ( $n = 3$ ) mice. Error bars indicate  $\pm$  SD. (C) Relative number of TH-positive neurons in the midbrain of *Mfn2<sup>DA</sup>* mice at 5 weeks of age. Open bars, control ( $n = 3$ ); filled bars, knockout ( $n = 3$ ) mice. Error bars indicate  $\pm$  SD.

corresponding to that of the enlarged mitochondria visualized by light microscopy (Fig. 3B). We observed no neurofibrillary tangles by electron microscopy of *Mfn2<sup>DA</sup>* neurons.

The profound mitochondrial morphological abnormalities motivated us to use an enzyme histochemical approach to simultaneously assess the activities of cytochrome *c* oxidase (COX) and succinate dehydrogenase (SDH). This COX/SDH assay showed a marked reduction in COX activity and increased SDH activity in midbrain DA neurons of *Mfn2<sup>DA</sup>* mice at 5 weeks of age (Fig. 4A), demonstrating that the abnormal mitochondrial morphology (Fig. 3B–D) was accompanied by severe respiratory chain deficiency. The vast majority of mitochondria in striatum are derived from non-DA nerve fibers and cells, and it is therefore not meaningful to perform COX/SDH staining in striatum of the *Mfn2<sup>DA</sup>* mice. No difference in COX/SDH histochemistry was seen in *Mfn1<sup>DA</sup>* mice (data not shown).

Parkin has been reported to have a role in the clearance of defective mitochondria *in vitro* (25,26), and we, therefore, investigated whether the respiratory chain-deficient mitochondria in *Mfn2<sup>DA</sup>* mice would recruit Parkin. We performed stereotaxic injections of adeno-associated virus (AAV) encoding mCherry-Parkin into the midbrain of *Mfn2<sup>DA</sup>* and control mice that both also expressed mito-YFP. We obtained robust cytoplasmic expression of mCherry-Parkin in a subset of DA neurons in *Mfn2<sup>DA</sup>* and control mice (Fig. 4B), but there was no recruitment of Parkin to the defective mitochondria in the *Mfn2<sup>DA</sup>* mice. Some neurons showed focal dots of strong cytoplasmic mCherry-Parkin expression, but these dots did not colocalize with mitochondria and were possibly caused by protein aggregation associated with the high mCherry-Parkin expression.

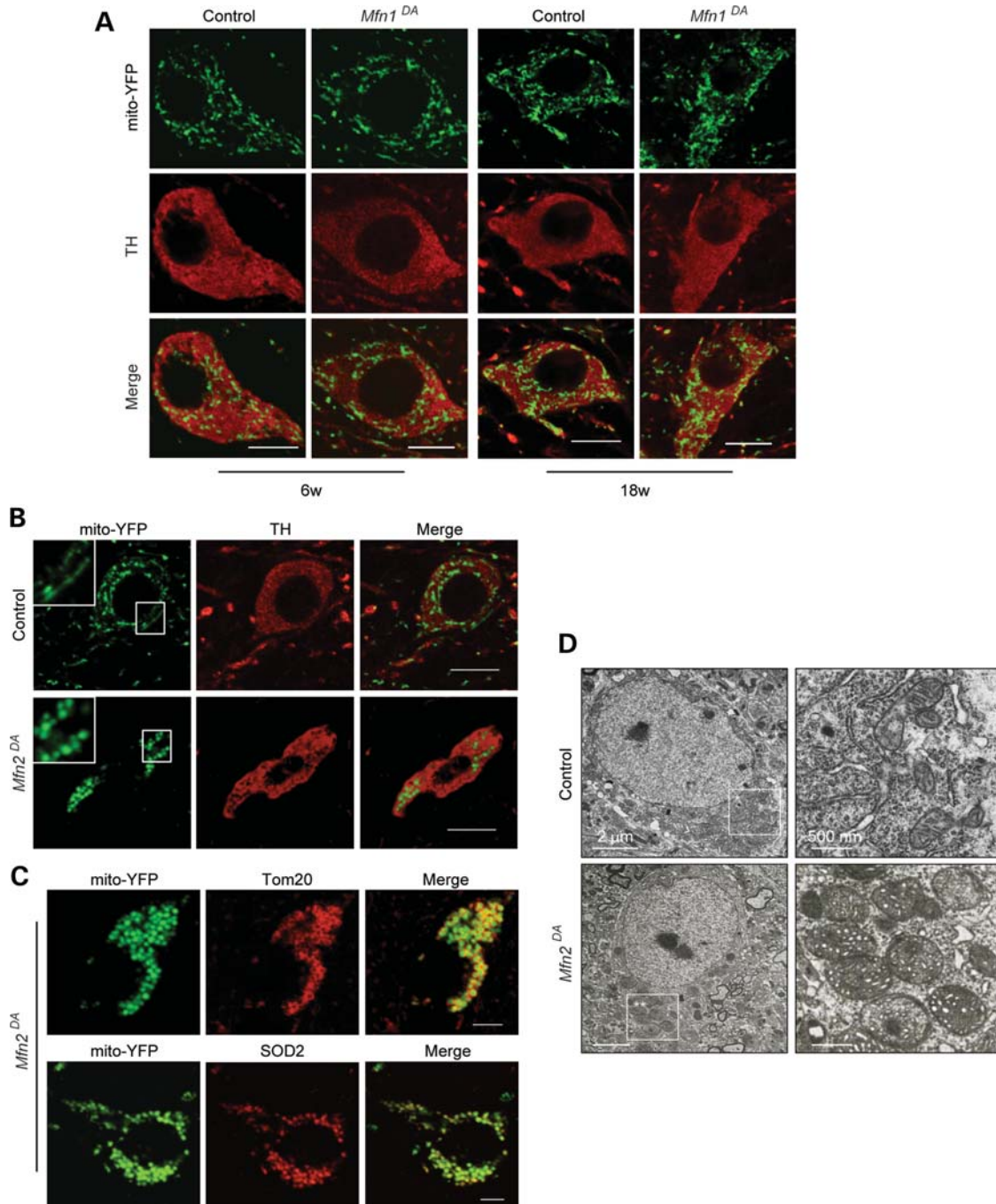


**Figure 3.** Mitochondrial morphology in Mfn1- and Mfn2-deficient DA neurons. (A) Confocal microscopy of YFP-labeled mitochondria in Mfn1-deficient DA neurons (genotype *Mfn1<sup>loxP</sup>/Mfn1<sup>loxP</sup>; +/DAT-cre; +/ROSA26<sup>SmY</sup>*) at 6 (n = 3) and 18 (n = 2) weeks of age (scale bar: 10 μm). (B) Mitochondrial morphology in DA neurons of control and Mfn2-deficient mice (genotype *Mfn2<sup>loxP</sup>/Mfn2<sup>loxP</sup>; +/DAT-cre; +/ROSA26<sup>SmY</sup>*) at 5 weeks of age (n = 5–7). YFP-labeled mitochondria in TH immunoreactive neurons (red) were analyzed (scale bar: 10 μm). (C) Confocal microscopy of YFP-labeled mitochondria in Mfn2-deficient DA neurons at 5 weeks of age. Mitochondria were double-labeled with antibodies against the mitochondrial outer membrane protein TOM20 (upper panel, red) or the mitochondrial matrix protein SOD2 (lower panel, red) (scale bar: 5 μm). (D) Mitochondria in 5-week-old control and Mfn2-deficient DA neurons were analyzed by electron microscopy (n = 2).

### Loss of targeting of DA axons to the striatum in the absence of Mfn2

*Mfn1<sup>DA</sup>* mice had no cell loss in SNc (Fig. 2B) and maintained a normal DA innervation of the striatum (Fig. 5A and B). Likewise, there was no decrease in the number of TH-positive

cell bodies in SNc in 5-week-old *Mfn2<sup>DA</sup>* mice (Fig. 2C), although the somata displayed pathological alterations, such as irregular margins and elongated nuclei (Fig. 3B and C). Strikingly, the *Mfn2<sup>DA</sup>* mice showed a profound lack of DA innervation (88% reduction) in the striatum (Fig. 5C and D). We

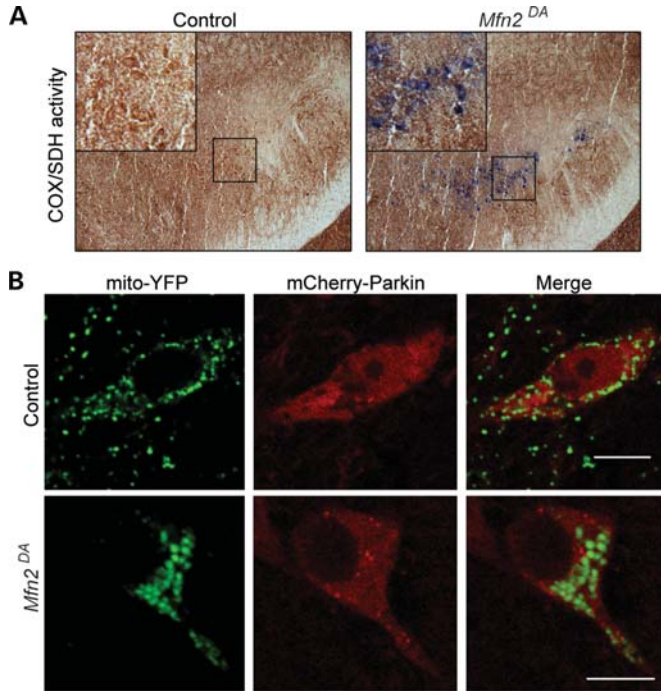


**Figure 4.** Dysfunctional mitochondria in *Mfn2*-deficient DA neurons do not recruit Parkin. **(A)** COX and SDH activity in control and *Mfn2*-deficient DA neurons at 5 weeks of age. Increased blue staining indicates decreased COX activity and increased SDH activity. **(B)** Stereotaxic delivery of AAV encoding mCherry-Parkin to midbrain DA neurons expressing mito-YFP in *Mfn2*<sup>DA</sup> mice at 4 weeks of age ( $n = 3$ ). Cells were analyzed 7 days after injections (scale bar: 10  $\mu$ m).

measured levels of DA and its major metabolites in different brain regions by high-performance liquid chromatography (HPLC) and found no significant differences in *Mfn1*<sup>DA</sup> mice at 50 weeks of age (Fig. 6A–C). In contrast, we found a severe reduction in DA in the striatum of *Mfn2*<sup>DA</sup> mice at 5 weeks of age (Fig. 6D). We also found increased 3,4-dihydroxyphenylacetic acid (DOPAC)/DA and of homovanillic acid (HVA)/DA ratios in *Mfn2*<sup>DA</sup> mice (Fig. 6E), as typically seen in DA-deficient states. The levels of serotonin [5-hydroxytryptamine creatinine sulfate (5-HT)] were increased in the striatum (Fig. 6F), possibly due to increased levels of trophic factors following the DA fiber denervation. Such increase is also seen in rats denervated by 6-hydroxydopamine in the neonatal period (27). The DA levels in SNc of *Mfn2*<sup>DA</sup> mice (Fig. 6G) were also decreased, which may be explained by the observed respiratory chain deficiency (Fig. 4A). Thus, *Mfn2* is critical for striatal projections of DA neurons and maintenance of DA homeostasis.

#### Loss of distal axonal mitochondria

We analyzed the number of YFP-labeled mitochondria in the dorsolateral striatum and found a profound reduction (89% reduction) in *Mfn2*<sup>DA</sup> mice (Fig. 7A and B). *Mfn1*<sup>DA</sup> mice showed no reduction in mitochondrial population in the striatum (Supplementary Material, Fig. S4A and B). The MitoPark mice have a parallel reduction in the amount of TH expressing DA fibers in the striatum and the amount of

mitochondria supplied by the DA nerve cell bodies (7). Similarly, also the *Mfn2*<sup>DA</sup> mice showed no difference in the relative amount of DA neuron-derived mitochondria in the striatum after normalization to the amount of TH-positive nerve fibers (Fig. 7C). Notably, the type of abnormal large round mitochondria found in the DA cell bodies of *Mfn2*<sup>DA</sup> mice were not noted in the few TH-positive striatal fibers.

#### DISCUSSION

High energy demands and the requirement to maintain cellular homeostasis at sites distant to the cell body likely make neurons particularly vulnerable to mitochondrial dysfunction. There is emerging evidence that degeneration of axons may occur independently and by mechanisms distinct from those of the cell body and that loss of dopaminergic axons is an early event in the progression of PD (28). This phenomenon is illustrated in *Mfn2*<sup>DA</sup> mice, where we find that loss of *Mfn2* has a profound effect on DA innervation of the striatum at a time point when the DA nerve cells in SNc are respiratory chain deficient, but still viable. A progressive loss of nigro-striatal projections, which precedes that of DA cell bodies, is also seen in a similar model with disruption of *Mfn2* in its DA neurons (29). Consistent with these observations, it has been reported that the overexpression of mutant forms of the *Mfn2* protein, which cause hereditary motor and sensory neuropathy, leads to axonal degeneration and impaired mitochondrial movement without loss of cell bodies in cultured neurons (30). Axon terminals are diminished already in very young ( $\sim 3.5$  weeks old) *Mfn2*<sup>DA</sup> mice, which suggest the occurrence of axonal degeneration in early postnatal life or impaired formation during development. The DA-containing nigrostriatal system appears around embryonic day E13 in rats and mice (31,32), but the formation of a terminal DA-containing dense network in the striatum is largely a postnatal event that takes place during the first 4 weeks of life in rodents (33,34). It is possible that loss of *Mfn2* impairs axon development during this period by preventing axonal transport of mitochondria. We have previously shown that mitochondrial dysfunction impairs anterograde supply of mitochondria in DA neurons (7) and *Mfn2* has also been reported to play a direct role in axonal transport of mitochondria (35), in addition to its role in fusion that is required to maintain respiratory chain function.

Although the number of SNc DA neurons is intact in *Mfn2*<sup>DA</sup> mice, mitochondria in the soma appear as separate, respiratory chain-deficient organelles. Such a condition should promote Parkin-mediated mitochondrial degradation (17). However, we were unable to detect any *in vivo* translocation of Parkin to these aberrant mitochondria. A possible explanation is that the mitochondrial membrane potential is maintained above the threshold required for Parkin translocation, as previously discussed in the context of the MitoPark mice, that also display no *in vivo* recruitment of Parkin to the enlarged and severely respiratory chain-deficient mitochondria (7).

It remains unclear why two homologous mitofusins have evolved in mammals. *Mfn1* and *Mfn2* can functionally replace each other to maintain mitochondrial fusion *in vitro*, but both genes are critical for embryonic development (10).

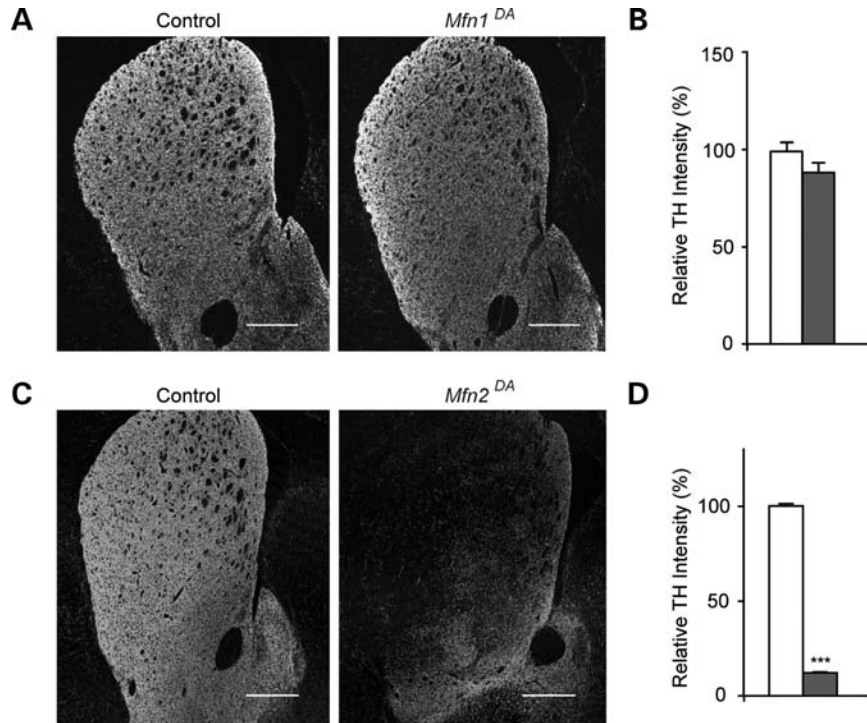


**Figure 5.** Nigrostriatal DA system in the striatum of *Mfn1*<sup>DA</sup> and *Mfn2*<sup>DA</sup> mice. (A) DA nerve terminals in the striatum of control and *Mfn1*<sup>DA</sup> mice were labeled by TH immunohistochemistry at 6 weeks of age (scale bar: 500  $\mu$ m). (B) Relative intensity of TH immunoreactivity. Open bar, control; filled bar, *Mfn1*<sup>DA</sup> mice ( $n = 3$  for each genotype). (C) TH-immunoreactive DA nerve terminals in the striatum in 5 weeks old control and *Mfn2*<sup>DA</sup> mice (scale bar: 500  $\mu$ m). (D) Intensity of TH immunoreactivity in the dorsolateral striatum. Open bar, control; filled bar, *Mfn2*<sup>DA</sup> mice ( $n = 3$  for each genotype). \*\*\* $P < 0.001$  by Student's two-tailed  $t$ -test.

Despite similar expression levels, we find a striking discrepancy between loss of *Mfn1* and *Mfn2* in DA neurons. Whereas loss of *Mfn2* causes abnormal mitochondrial morphology, respiratory chain dysfunction and severe lack of DA terminals in the striatum, loss of *Mfn1* does not significantly affect DA neuron survival or function. However, preliminary results indicate that DA-specific *Mfn1* and *Mfn2* double-knockout mice have an even shorter lifespan than the *Mfn2*<sup>DA</sup> mice, suggesting a partial suppression of the *Mfn2* knockout phenotype by *Mfn1*. These findings are similar to reports of the disruption of *Mfn1* and *Mfn2* in cerebellar Purkinje cells. Also here, the neurons are largely unaffected by the loss of *Mfn1*, whereas loss of *Mfn2* causes a profound neurodegeneration (11). It thus seems likely that *Mfn2* has an additional role in neurons besides promoting mitochondrial fusion. For example, *Mfn2* may be of particular importance for axonal transport of mitochondria (35) and has also been reported to mediate the interaction between mitochondria and the endoplasmic reticulum (36).

In summary, our results demonstrate that mammalian DA neurons *in vivo* critically depend on *Mfn2*, but not *Mfn1*, to maintain mitochondrial morphology, axon integrity and DA-mediated motor control. A picture is now emerging from experimental mouse work that argues that mitochondrial dysfunction preferentially affects the DA innervation of the striatum by impairing axonal targeting, as demonstrated in this paper, mitochondrial axonal transport (4,7) or release of DA from nerve terminals in the striatum (37). These experimental findings shed important new light on the possible

role of mitochondrial dysfunction in PD and are consistent with observations that the DA neuron pathology in human PD patients starts peripherally with the degeneration of the striatal DA nerve terminals (28).

## MATERIALS AND METHODS

### Breeding of mice

Mice with loxP-flanked *Mfn1* or *Mfn2* alleles were obtained from Taconic and crossed with *DAT-cre* mice (4). The resulting double heterozygous offspring were, in turn, crossed with homozygous *Mfn1*<sup>loxP</sup>/*Mfn1*<sup>loxP</sup> or *Mfn2*<sup>loxP</sup>/*Mfn2*<sup>loxP</sup> mice to generate DA-specific knockouts for *Mfn1* (*Mfn1*<sup>loxP</sup>/*Mfn1*<sup>loxP</sup>; +/*DAT-cre*) or *Mfn2* (*Mfn2*<sup>loxP</sup>/*Mfn2*<sup>loxP</sup>; +/*DAT-cre*), respectively. In a subset of matings, the *Gt(ROSA26)Sor*<sup>Stop-mito-YFP</sup> allele (7) was introduced by an additional cross in the parental generation.

Mice were fed *ad libitum* (R70 Standard Diet; Lactamin), had free access to water and were kept on a 12:12 h light:dark cycle at 24°C. Experiments were approved by the Animal Ethics Committee of the North Stockholm region and conducted in accordance with international standards on animal welfare and Swedish law.

### RNA expression analysis

Total RNA was extracted from heart samples using TRIzol (Invitrogen). Reverse transcription was conducted on 2  $\mu$ g of

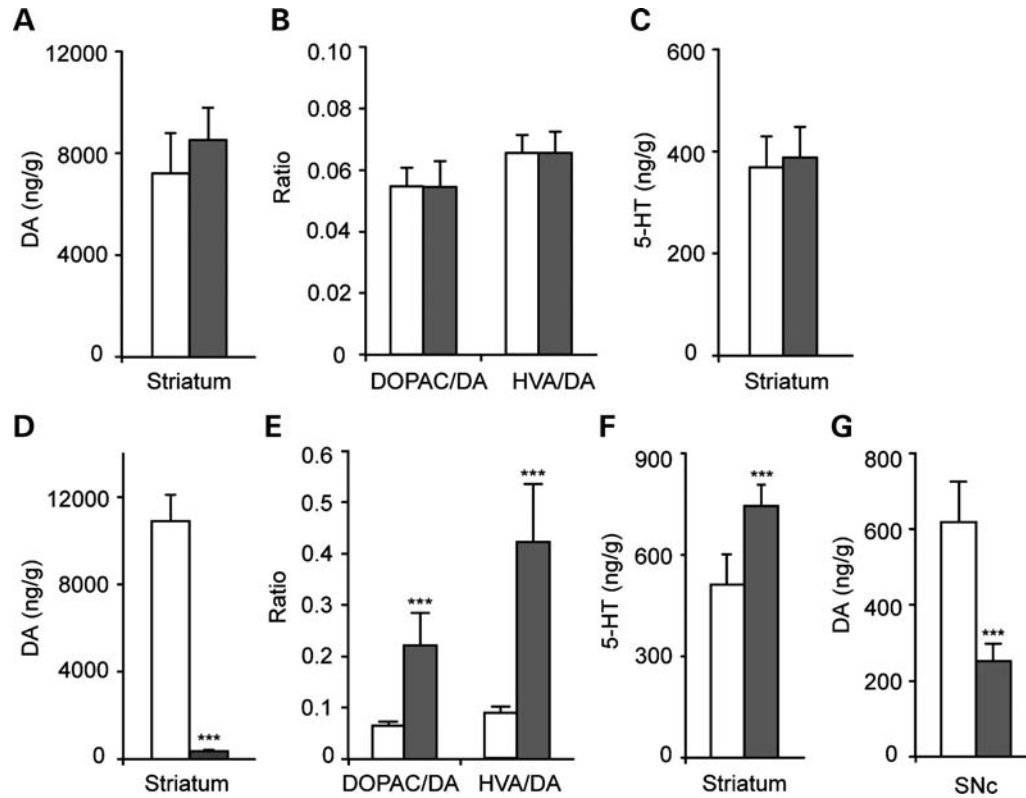


**Figure 6.** DA homeostasis in *Mfn1<sup>DA</sup>* and *Mfn2<sup>DA</sup>* mice. (A) Levels of DA in the striatum of *Mfn1<sup>DA</sup>* mice at 50 weeks of age. (B) DOPAC:DA and HVA:DA ratios in the striatum of *Mfn1<sup>DA</sup>* mice. (C) Levels of 5-HT in the striatum. Open bars, control; filled bars, *Mfn1<sup>DA</sup>* mice. (D) Levels of DA in the striatum of *Mfn2<sup>DA</sup>* mice. (E) Ratios of DOPAC:DA and HVA:DA in the striatum. (F) Levels of 5-HT in the striatum. (G) Levels of DA in SNc. The measurements in (D)–(G) show levels in control (open bars) and *Mfn2<sup>DA</sup>* (filled bars) mice at 5 weeks of age. Data shown as the mean  $\pm$  SD. \*\*\* $P < 0.001$  by Student's two-tailed  $t$ -test ( $n = 7$  for each genotype).

total RNA by using the high-capacity cDNA reverse transcription kit (Applied Biosystems). Semi-quantitative real-time polymerase chain reaction was subsequently performed using specific TaqMan probes for the *Mfn1* and *Mfn2* transcripts (Mm01289372\_m1 and Mm00500120\_m1 gene expression assays, Applied Biosystems). The transcript levels were normalized to  $\beta$ -2 microglobulin RNA (Mm00437762\_m1 gene expression assay, Applied Biosystems).

### Behavior analysis

Mice were analyzed at 5 weeks of age ( $n = 17$ ) using an animal activity monitoring system (VersaMax, AccuScan Instruments). Following habituation to the dimly lit, low-noise and ventilated experimental room for at least 30 min, mice were placed individually in activity cages (40  $\times$  40 and 30 cm high). A grid of infrared light beams at floor level and 7.5 cm above recorded spontaneous horizontal and vertical activities, respectively, over a period of 1.5 h during the light phase (between 4 and 6 p.m.).

### In situ hybridization

To detect the expression of gene transcripts, the following oligonucleotide probes were used: TH, 5'-GGT GTG CAG CTC ATC CTG GAC CCC CTC CAA GGA GCG CT-3'; *Mfn1*, 5'-AAC GCT CTC TCT TTC GCA CGG GTC GTC

CAC GTC AGC CTC TCA TAA AGG TA-3' and *Mfn2*, 5'-ACT GTC CCA GCA AAA AGG GTA TGA GGG GCG AGT GAG CAC AAG-3'. Probes were labeled with  $^{33}\text{P}$ , as described (38).

### Immunohistochemistry and microscopy

Mice were perfused with  $\text{Ca}^{2+}$ -/ $\text{Mg}^{2+}$ -free Tyrode's solution followed by 4% paraformaldehyde with 0.4% picric acid in 0.16 M phosphate buffer. The brains were dissected out, post-fixed for 2 h and equilibrated with 10% sucrose buffer containing 0.1% sodium azide. The brains were frozen on  $\text{CO}_2$  ice and cryosectioned to obtain 14 or 20  $\mu\text{m}$  sections. Rehydrated sections were immunolabeled overnight with primary antibodies against TH (1:500; Pel-Freez), Tom20 (1:400; Santa Cruz) and SOD2 (1:200; Upstate).

For non-fluorescent labeling, biotinylated secondary antibodies (1:400; Vector Laboratories) were used and detected using a peroxidase substrate (Vector SG, Vector Laboratories). For fluorescence labeling, Cy3-conjugated secondary antibodies (1:400; Jackson Biolabs) were used. Confocal images were acquired by sequential scanning using an LSM510 Meta microscope (Zeiss). YFP was excited with the 514 nm argon laser and emission was detected at 520–542 nm. Cy3 and mCherry were excited with a 543 nm helium-neon laser and detected at 553–649 and 584–638 nm, respectively.

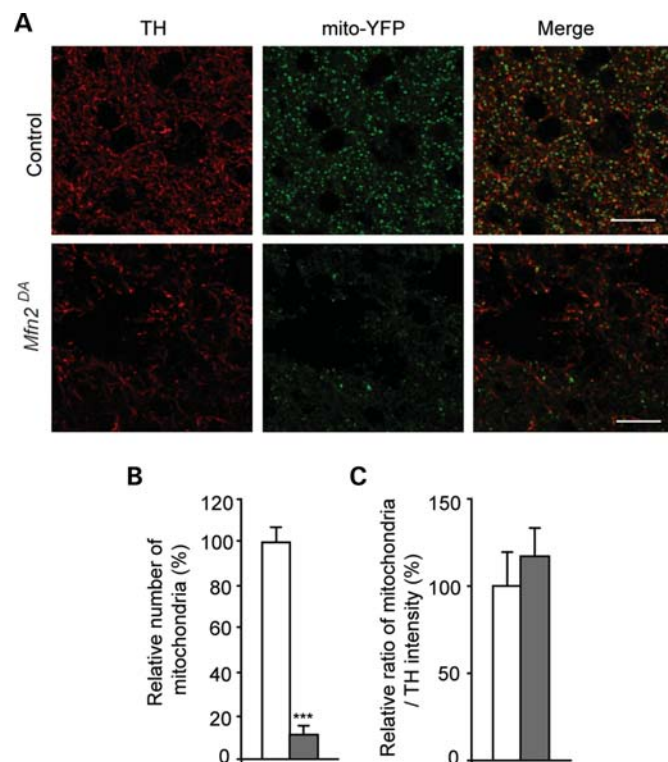


**Figure 7.** Lack of DA-neuron-derived mitochondria in the striatum of *Mfn2<sup>DA</sup>* mice. (A) YFP-labeled mitochondria in TH-positive nerve terminals in the striatum of control and *Mfn2<sup>DA</sup>* mice (scale bars: 10 μm). (B) Relative number of mitochondria in the striatum of control and *Mfn2<sup>DA</sup>* mice at the age of 5 weeks. (C) Relative amount of mitochondria normalized to TH density in the striatum. Open bars, control; filled bars, *Mfn2<sup>DA</sup>* mice. Error bars represent ± SD. \*\*\**P* < 0.001 by Student's two-tailed *t*-test (*n* = 3).

### Stereology

Coronary midbrain cryosections (20 μm thickness) were thawed and every sixth section was immunolabeled for TH. SNc was outlined as described (39). A microscope with a motorized stage (Nikon E600) controlled by stereology software (Stereologer, SRC; version 2001) was used for design-based stereology. SNc was outlined using a 4× objective and cells counted using a 60×/1.4NA oil objective. Counting frames were spaced 200 μm apart. A coefficient of error of <0.1 was accepted.

### Image analysis and quantifications

ImageJ was used for the measurement of TH density in the striatum. For the quantification of striatal mitochondria, images were obtained using a 40× objective. The MeasurementPro module of Imaris imaging software (Bitplane) was used to calculate the number of mitochondrial dots in the striatum.

### Measurements of monoamines

The brains (*n* = 7 per genotype) were rapidly dissected, chilled in ice-cold saline and bilateral pieces of the striatum, midbrain and frontal cortex dissected and frozen on dry ice. Tissue pieces were weighed and homogenized by sonication in 0.1 M perchloric acid containing 0.4 mM sodium bisulfite followed by

centrifugation and filtration of the supernatant. Noradrenalin, DA, DOPAC, HVA and 5-HT in the supernatants were separated by HPLC on a reverse-phase column (Reprosil-Pur, C18-AQ 150 × 4 mm, 5 μm particle diameter; Dr Maisch HPLC GmbH) with a mobile phase of a 0.05 M sodium phosphate/0.03 M citric acid buffer containing 0.1 mM ethylenediaminetetraacetic acid, with various amounts of methanol and sodium-1-octane sulfonic acid. Monoamine levels were measured by electrochemical detection as previously described (37) and expressed as ng/g wet weight of tissue.

### Electron microscopy

Mice were perfused with 2% glutaraldehyde in 440 mM Millonig's buffer (pH 7.4). The brains were removed and a 1-mm-thick coronal section containing the SNc dissected. The SNc of each side was trimmed from the surrounding tissue and cut to generate three pieces of 1–2 mm<sup>3</sup> that were further post-fixed in 2% glutaraldehyde solution. The specimens were further trimmed, osmicated, dehydrated and embedded in Durcupan (Fluka, Buchs, Switzerland). Ultrathin sections from SN were collected on formvar-coated copper grids, contrasted with uranyl acetate and lead citrate and examined by electron microscopy (CM12; Philips, Eindhoven, the Netherlands).

### Stereotactic injections

Mice anesthetized with isoflurane and buprenorphine (0.075 mg/kg s.c.) were put in a stereotactic frame (Stoelting). A midline skin incision was made and a burr hole was made over each side of the midbrain. Viral constructs (1 × 10<sup>9</sup> viral genomes in 2 μl) were injected just above SNc (2.9 mm caudal to bregma, 1.3 mm lateral to the midline and 4.2 mm ventral to dura mater) using a 10 μl Hamilton syringe with a custom-made 33G needle (45° type 4 tip). A microsyringe pump controller (World Precision Instruments) was used to deliver the volume at a speed of 300 nl/min. The needle was left *in situ* another 4 min prior to retraction. The scalp was closed using a 6-0 Ethicon suture.

### Statistical analysis

The error bars on figures represent the mean ± SD of all determinations. Two-tailed unpaired *t*-tests were used to assess statistical significance in figures with \**P* < 0.05, \*\**P* < 0.01 and \*\*\**P* < 0.001, respectively. Statistics were performed using appropriate software (GraphPad Prism version 5.0; GraphPad Software Inc.).

### SUPPLEMENTARY MATERIAL

Supplementary Material is available at *HMG* online.

### ACKNOWLEDGEMENTS

We thank Eva Lindqvist, Karin Lundströmer and Karin Pernold for technical assistance, Dagmar Galter and Anita Bergstrand for assistance with electron microscopy and Marie Olofsson Westerlund for advice with *in situ* hybridization.

**Conflict of Interest statement.** None declared.

## FUNDING

This work was supported by the Swedish Research Council (K2011-62X-21870-01-6, K2009-61X-03185-39-3); Swedish Brain Power; Parkinsonsfonden, Sweden; Hjärnfonden, Sweden and the Karolinska Institute (DPA). Funding to pay the Open Access publication charges for this article was provided by Vetenskapsrådet.

## REFERENCES

- Schapiro, A.H. (2008) Mitochondrial dysfunction in neurodegenerative diseases. *Neurochem. Res.*, **33**, 2502–2509.
- Narendra, D.P., Jin, S.M., Tanaka, A., Suen, D.F., Gautier, C.A., Shen, J., Cookson, M.R. and Youle, R.J. (2010) PINK1 is selectively stabilized on impaired mitochondria to activate Parkin. *PLoS Biol.*, **8**, e1000298.
- Pils, A. and Winklhofer, K.F. (2012) Parkin, PINK1 and mitochondrial integrity: emerging concepts of mitochondrial dysfunction in Parkinson's disease. *Acta Neuropathol.*, **123**, 173–188.
- Ekstrand, M.I., Terzioglu, M., Galter, D., Zhu, S., Hofstetter, C., Lindqvist, E., Thams, S., Bergstrand, A., Hansson, F.S., Trifunovic, A. *et al.* (2007) Progressive parkinsonism in mice with respiratory-chain-deficient dopamine neurons. *Proc. Natl Acad. Sci. USA*, **104**, 1325–1330.
- Kukat, C., Wurm, C.A., Spahr, H., Falkenberg, M., Larsson, N.G. and Jakobs, S. (2011) Super-resolution microscopy reveals that mammalian mitochondrial nucleoids have a uniform size and frequently contain a single copy of mtDNA. *Proc. Natl Acad. Sci. USA*, **108**, 13534–13539.
- Hallberg, B.M. and Larsson, N.G. (2011) TFAM forces mtDNA to make a U-turn. *Nat. Struct. Mol. Biol.*, **18**, 1179–1181.
- Sterky, F.H., Lee, S., Wibom, R., Olson, L. and Larsson, N.G. (2011) Impaired mitochondrial transport and Parkin-independent degeneration of respiratory chain-deficient dopamine neurons in vivo. *Proc. Natl Acad. Sci. USA*, **108**, 12937–12942.
- Hoppins, S., Lackner, L. and Nunnari, J. (2007) The machines that divide and fuse mitochondria. *Annu. Rev. Biochem.*, **76**, 751–780.
- Chan, D.C. (2006) Mitochondrial fusion and fission in mammals. *Annu. Rev. Cell Dev. Biol.*, **22**, 79–99.
- Chen, H., Detmer, S.A., Ewald, A.J., Griffin, E.E., Fraser, S.E. and Chan, D.C. (2003) Mitofusins Mfn1 and Mfn2 coordinately regulate mitochondrial fusion and are essential for embryonic development. *J. Cell Biol.*, **160**, 189–200.
- Chen, H., McCaffery, J.M. and Chan, D.C. (2007) Mitochondrial fusion protects against neurodegeneration in the cerebellum. *Cell*, **130**, 548–562.
- Chen, H., Vermulst, M., Wang, Y.E., Chomyn, A., Prolla, T.A., McCaffery, J.M. and Chan, D.C. (2010) Mitochondrial fusion is required for mtDNA stability in skeletal muscle and tolerance of mtDNA mutations. *Cell*, **141**, 280–289.
- Delettre, C., Lenaers, G., Pelloquin, L., Belenguer, P. and Hamel, C.P. (2002) OPA1 (Kjer type) dominant optic atrophy: a novel mitochondrial disease. *Mol. Genet. Metab.*, **75**, 97–107.
- Zuchner, S., Mersyanova, I.V., Muglia, M., Bissar-Tadmouri, N., Rochelle, J., Dadali, E.L., Zappia, M., Nelis, E., Patitucci, A., Senderek, J. *et al.* (2004) Mutations in the mitochondrial GTPase mitofusin 2 cause Charcot-Marie-Tooth neuropathy type 2A. *Nat. Genet.*, **36**, 449–451.
- Twig, G., Elorza, A., Molina, A.J., Mohamed, H., Wikstrom, J.D., Walzer, G., Stiles, L., Haigh, S.E., Katz, S., Las, G. *et al.* (2008) Fission and selective fusion govern mitochondrial segregation and elimination by autophagy. *EMBO J.*, **27**, 433–446.
- Youle, R.J. and Narendra, D.P. (2011) Mechanisms of mitophagy. *Nat. Rev. Mol. Cell Biol.*, **12**, 9–14.
- Narendra, D.P. and Youle, R.J. (2011) Targeting mitochondrial dysfunction: role for PINK1 and Parkin in mitochondrial quality control. *Antioxid. Redox Signal.*, **14**, 1929–1938.
- Westermann, B. (2010) Mitochondrial fusion and fission in cell life and death. *Nat. Rev. Mol. Cell Biol.*, **11**, 872–884.
- Tanaka, A., Cleland, M.M., Xu, S., Narendra, D.P., Suen, D.F., Karbowski, M. and Youle, R.J. (2010) Proteasome and p97 mediate mitophagy and degradation of mitofusins induced by Parkin. *J. Cell Biol.*, **191**, 1367–1380.
- Glauser, L., Sonnay, S., Stafa, K. and Moore, D.J. (2011) Parkin promotes the ubiquitination and degradation of the mitochondrial fusion factor mitofusin 1. *J. Neurochem.*, **118**, 636–645.
- Ziviani, E., Tao, R.N. and Whitworth, A.J. (2010) Drosophila Parkin requires PINK1 for mitochondrial translocation and ubiquitinates mitofusin. *Proc. Natl Acad. Sci. USA*, **107**, 5018–5023.
- Deng, H., Dodson, M.W., Huang, H. and Guo, M. (2008) The Parkinson's disease genes pink1 and parkin promote mitochondrial fission and/or inhibit fusion in *Drosophila*. *Proc. Natl Acad. Sci. USA*, **105**, 14503–14508.
- Poole, A.C., Thomas, R.E., Andrews, L.A., McBride, H.M., Whitworth, A.J. and Pallanck, L.J. (2008) The PINK1/Parkin pathway regulates mitochondrial morphology. *Proc. Natl Acad. Sci. USA*, **105**, 1638–1643.
- Wang, J., Wilhelmsson, H., Graff, C., Li, H., Oldfors, A., Rustin, P., Bruning, J.C., Kahn, C.R., Clayton, D.A., Barsh, G.S. *et al.* (1999) Dilated cardiomyopathy and atrioventricular conduction blocks induced by heart-specific inactivation of mitochondrial DNA gene expression. *Nat. Genet.*, **21**, 133–137.
- Narendra, D., Tanaka, A., Suen, D.F. and Youle, R.J. (2008) Parkin is recruited selectively to impaired mitochondria and promotes their autophagy. *J. Cell Biol.*, **183**, 795–803.
- Matsuda, N., Sato, S., Shiba, K., Okatsu, K., Saisho, K., Gautier, C.A., Sou, Y.S., Saiki, S., Kawajiri, S., Sato, F. *et al.* (2010) PINK1 stabilized by mitochondrial depolarization recruits Parkin to damaged mitochondria and activates latent Parkin for mitophagy. *J. Cell Biol.*, **189**, 211–221.
- Stachowiak, M.K., Bruno, J.P., Snyder, A.M., Stricker, E.M. and Zigmond, M.J. (1984) Apparent sprouting of striatal serotonergic terminals after dopamine-depleting brain lesions in neonatal rats. *Brain Res.*, **291**, 164–167.
- Cheng, H.C., Ulane, C.M. and Burke, R.E. (2010) Clinical progression in Parkinson disease and the neurobiology of axons. *Ann. Neurol.*, **67**, 715–725.
- Pham, A.H., Meng, S., Chu, Q.N. and Chan, D.C. (2012) Loss of Mfn2 results in progressive, retrograde degeneration of dopaminergic neurons in the nigrostriatal circuit. *Hum. Mol. Genet.*, **21**, 1093–1103.
- Misko, A.L., Sasaki, Y., Tuck, E., Milbrandt, J. and Baloh, R.H. (2012) Mitofusin2 mutations disrupt axonal mitochondrial positioning and promote axon degeneration. *J. Neurosci.*, **32**, 4145–4155.
- Golden, G.S. (1973) Prenatal development of the biogenic amine systems of the mouse brain. *Dev. Biol.*, **33**, 300–311.
- Olson, L. and Seiger, A. (1972) Early prenatal ontogeny of central monoamine neurons in the rat: fluorescence histochemical observations. *Z. Anat. Entwicklungsgesch.*, **137**, 301–316.
- Roffler-Tarlov, S. and Graybiel, A.M. (1987) The postnatal development of the dopamine-containing innervation of dorsal and ventral striatum: effects of the weaver gene. *J. Neurosci.*, **7**, 2364–2372.
- Seiger, A. and Olson, L. (1973) Late prenatal ontogeny of central monoamine neurons in the rat: fluorescence histochemical observations. *Z. Anat. Entwicklungsgesch.*, **140**, 281–318.
- Misko, A., Jiang, S., Wegorzewska, I., Milbrandt, J. and Baloh, R.H. (2010) Mitofusin 2 is necessary for transport of axonal mitochondria and interacts with the Miro/Milton complex. *J. Neurosci.*, **30**, 4232–4240.
- de Brito, O.M. and Scorrano, L. (2008) Mitofusin 2 tethers endoplasmic reticulum to mitochondria. *Nature*, **456**, 605–610.
- Sterky, F.H., Hoffman, A.F., Milenkovic, D., Bao, B., Paganelli, A., Edgar, D., Wibom, R., Lupica, C.R., Olson, L. and Larsson, N.G. (2012) Altered dopamine metabolism and increased vulnerability to MPTP in mice with partial deficiency of mitochondrial complex I in dopamine neurons. *Hum. Mol. Genet.*, **21**, 1078–1089.
- Dagerlind, A., Friberg, K., Bean, A.J. and Hokfelt, T. (1992) Sensitive mRNA detection using unfixed tissue: combined radioactive and non-radioactive in situ hybridization histochemistry. *Histochemistry*, **98**, 39–49.
- Baquet, Z.C., Williams, D., Brody, J. and Smeyne, R.J. (2009) A comparison of model-based (2D) and design-based (3D) stereological methods for estimating cell number in the substantia nigra pars compacta (SNpc) of the C57BL/6J mouse. *Neuroscience*, **161**, 1082–1090.